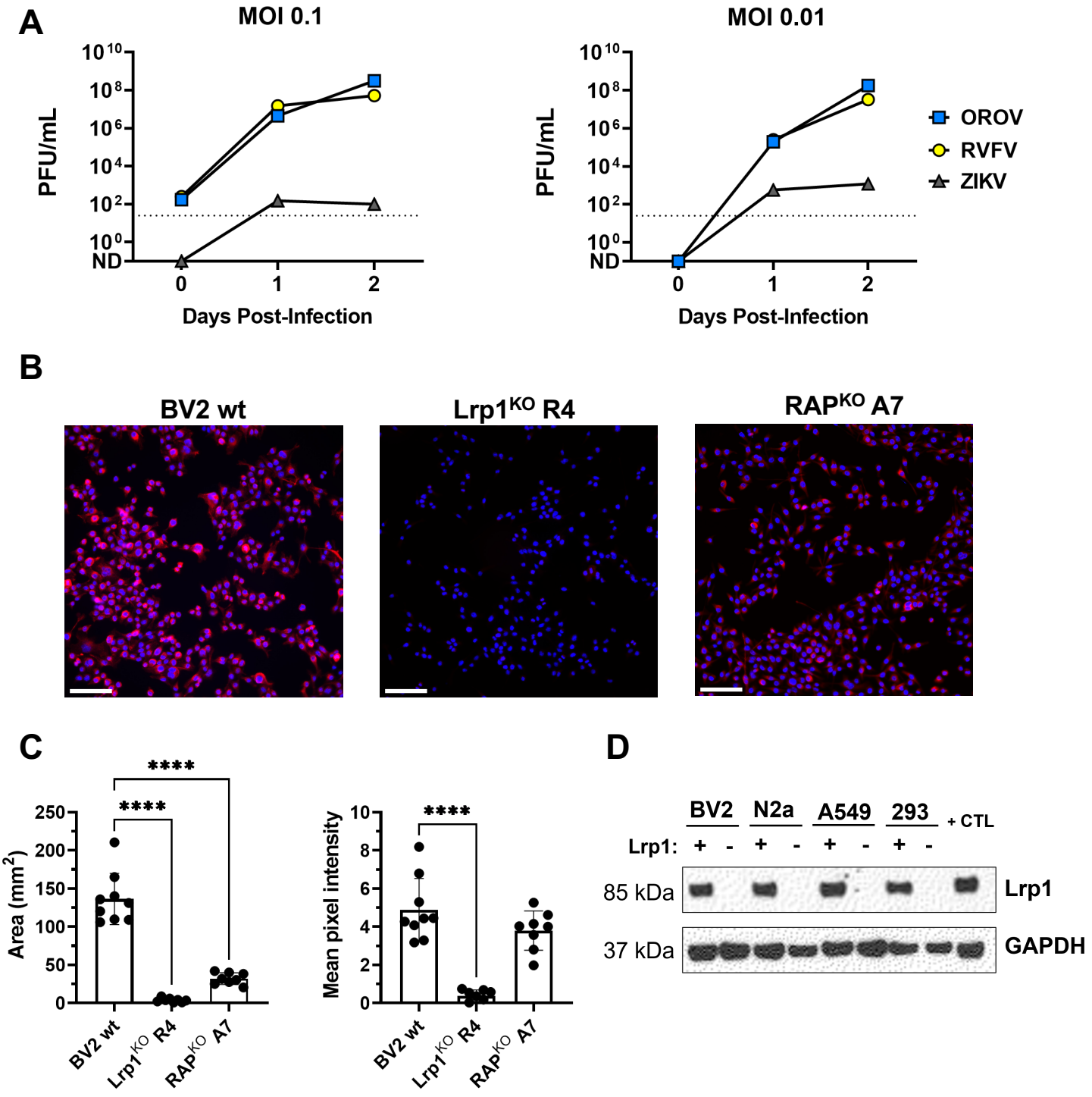

Fig. S1. OROV, RVFV, and ZIKV replication in BV2 cells and Lrp1^{KO} cell lines. (A) Growth of OROV, RVFV and ZIKV in wild-type mouse microglial BV2 cells at MOI 0.1 and MOI 0.01. Viral titers determined by plaque assay. (B) BV2 Lrp1^{KO} and RAP^{KO} cell lines described in Ganaie et al. 2021 show reduced expression of Lrp1 based on immunofluorescence with anti-Lrp1 mAb (20X). Scale is 50μm. (C) Image quantification of cells from panel (B) shows significantly less area (mm^2) and mean pixel intensity associated with Lrp1 staining in KO cell lines. (D) Western blot for Lrp1 demonstrating KO in BV2, N2a, A549, and HEK293T (293) cell lines. Positive control (+CTL) is homogenized C57BL/6J mouse liver. Statistical significance was determined using 2-way ANOVA. ****, p<0.0001.

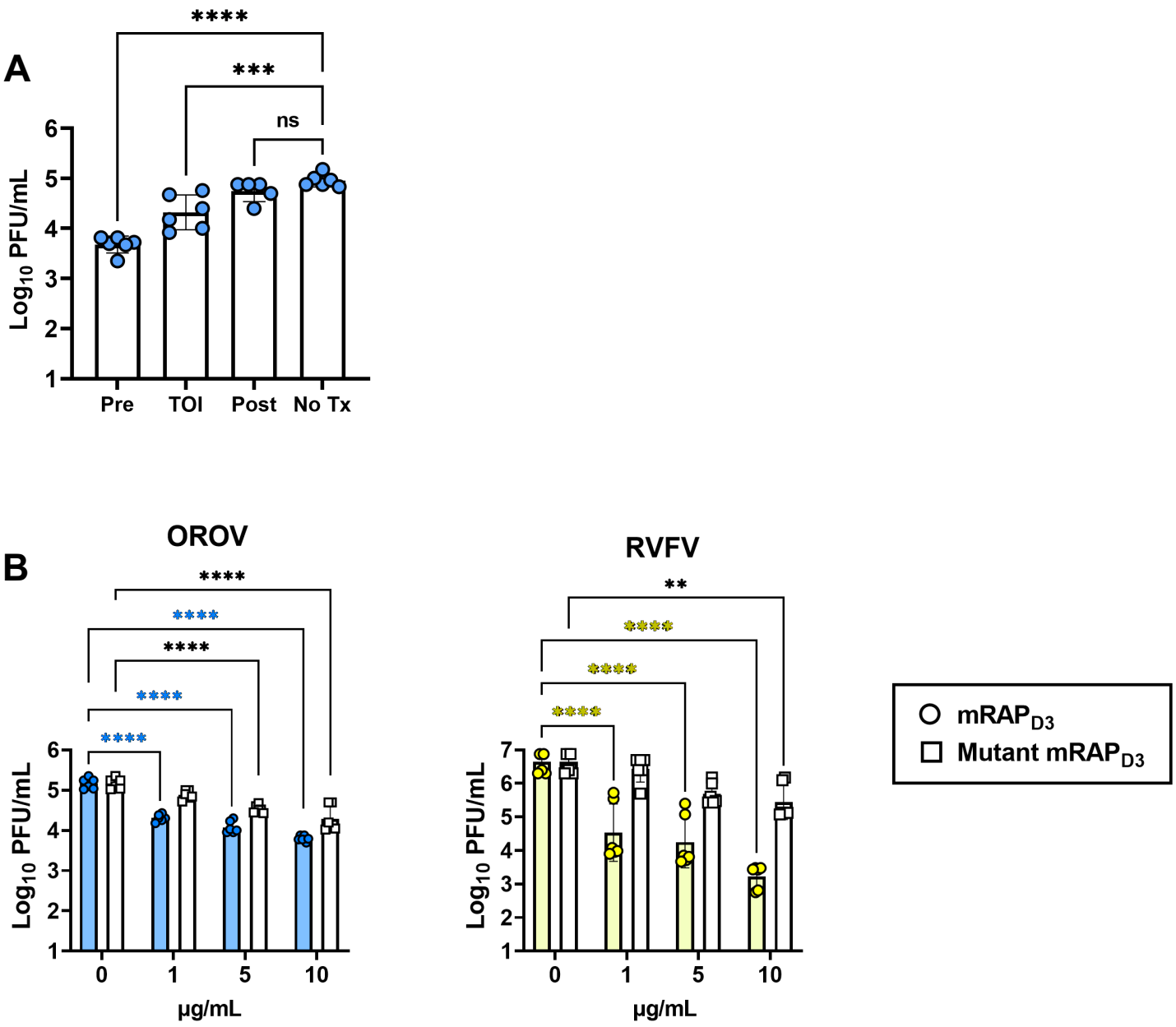

Fig S2. The Lrp1-binding chaperone RAP can inhibit OROV infection of Vero E6 cells and BV2 mouse microglia cells. (A) 10µg/mL mouse RAP D3 ($mRAP_{D3}$) was added to Vero E6 cells 1 hour prior to infection (Pre), at the time of infection (TOI), or after the infection (Post) with MOI 0.1 of OROV. Samples were harvested at 24 hpi and infectious virus was measured by viral plaque assay. (B) $mRAP_{D3}$ or mutant $mRAP_{D3}$ were added to BV2 cells 1 hour prior to infection with MOI 0.1 of OROV or RVFV. Samples were harvested at 24 hpi and infectious virus was measured by plaque assay. Statistical significance was determined using 1-way ANOVA or 2-way ANOVA on log-transformed data. Experiments were repeated two times. ***, $p<0.001$; ****, $p<0.0001$.

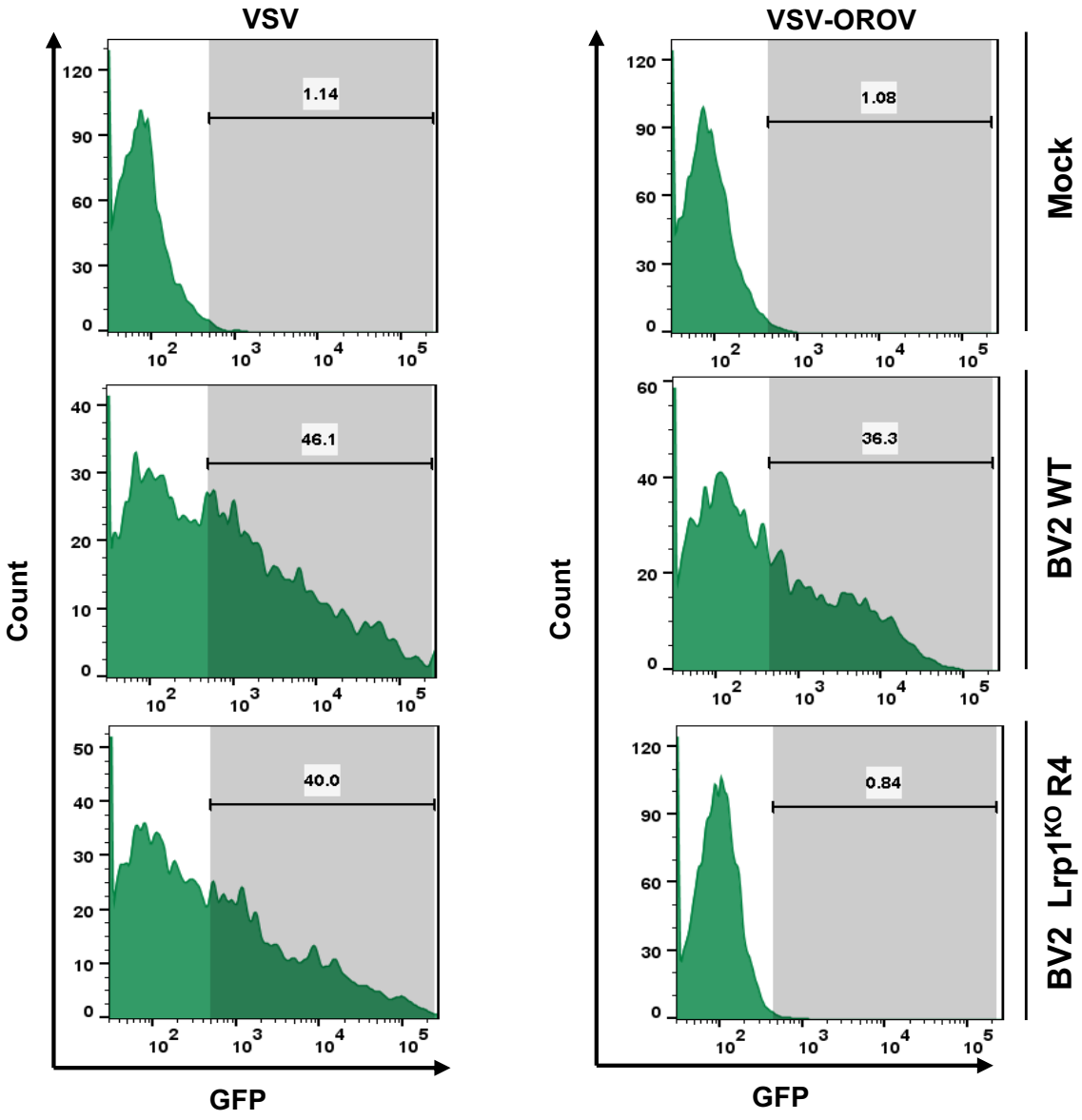

Fig. S3. VSV-OROV infection is reduced in BV2 Lrp1^{KO} R4 cells. Histograms showing GFP expression from VSV (MOI 1; left column) or VSV-OROV (MOI 5; right column) infection of BV2 wt and BV2 Lrp1^{KO} R4 cells. Samples were collected at 6 -8 hpi and processed by flow cytometry.

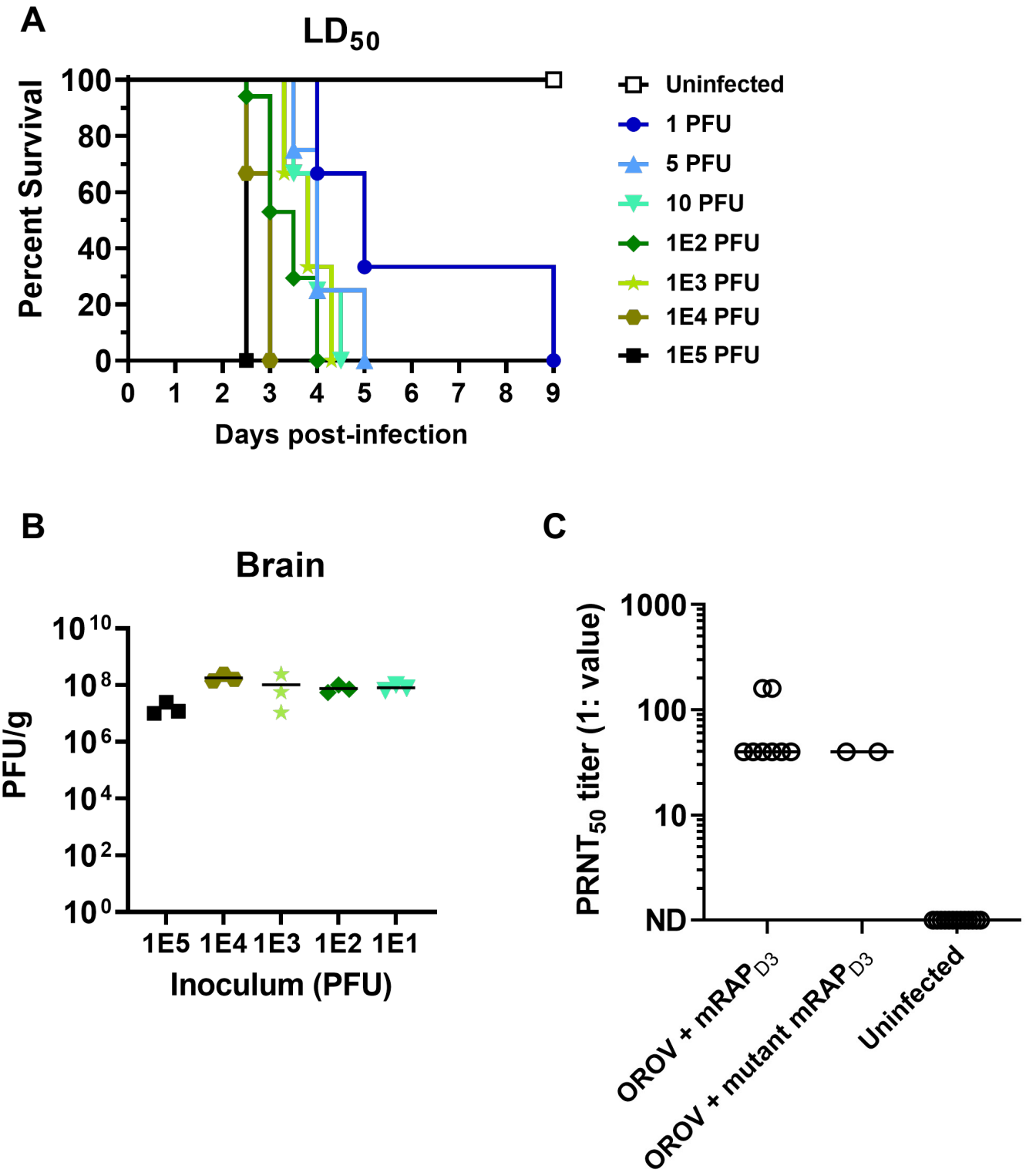

Fig. S4. Intracerebral OROV infection results in high brain titers regardless of dose, and survivors in the treated groups produce neutralizing antibodies by 10-15 dpi. (A) Seven doses of OROV were administered IC into 3–4-week-old C57BL/6J mice to determine a lethal dose. (B) Brain tissues were collected from mice in the OROV IC dosing experiment. Tissues were collected at time of death or euthanasia and were processed by viral plaque assay. (C) Endpoint dilutions on surviving $mRAP_{D3}$ and mutant $mRAP_{D3}$-treated, OROV-infected serum from 10 randomly selected mice. Uninfected controls were included for comparison. Experiments were repeated two times. Tx=treatment, Dpi=days post-infection.

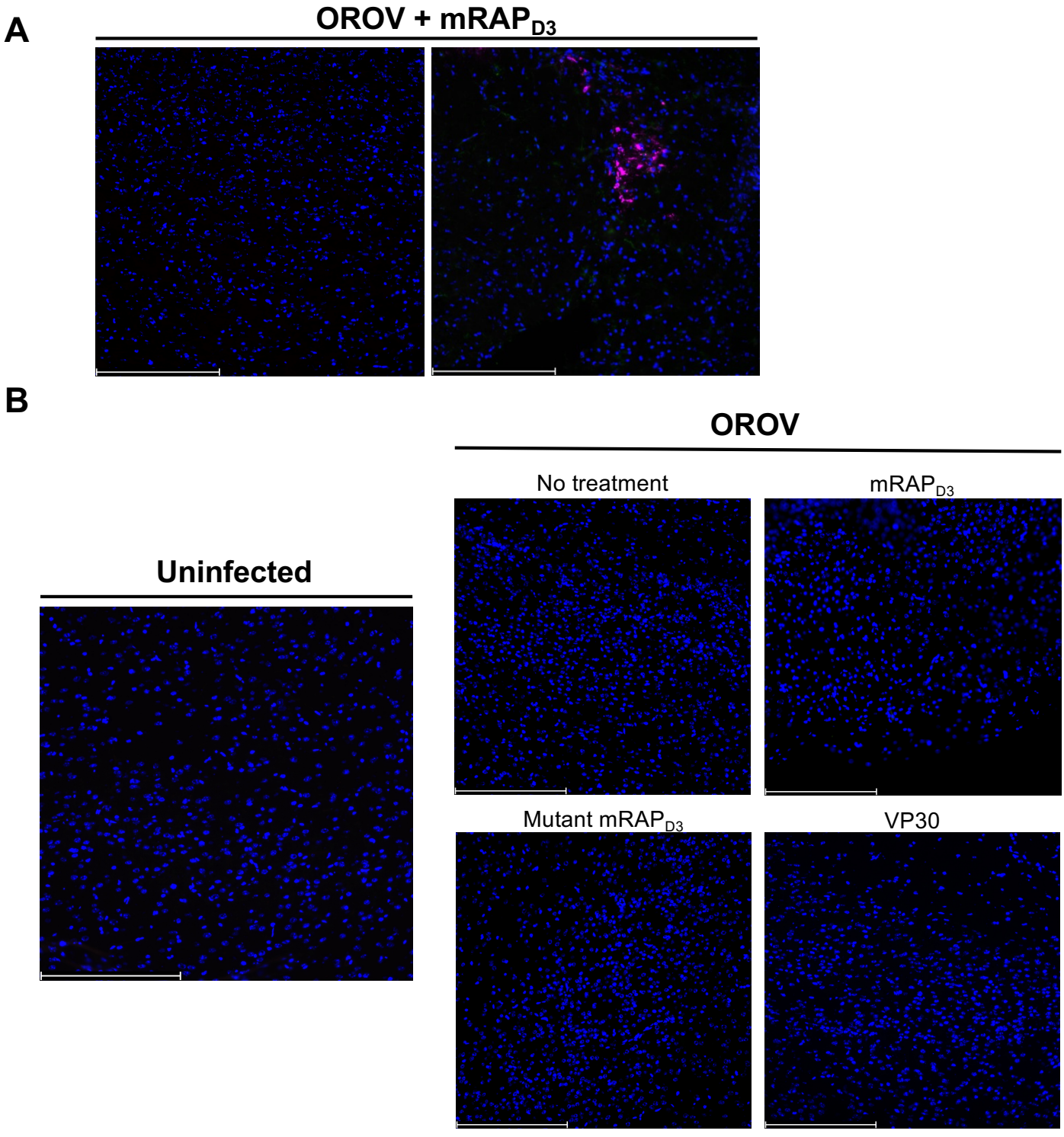

Fig. S5. Additional images of immunofluorescence microscopy from Fig. 6. (A) Additional representative images of brain tissue from OROV-infected, mRAPD3-treated mice at 3 dpi (20X). (B) Primary delete images for brain tissue from each experimental and control group (20X). Scale is 250μm.